

Spin adduct formation from lipophilic EMPO-derived spin traps with various oxygen- and carbon-centered radicals

Klaus Stolze^a, Natascha Udilova^a, Thomas Rosenau^b, Andreas Hofinger^b, Hans Nohl^{a,*}

^aResearch Institute of Pharmacology and Toxicology, University of Veterinary Medicine Vienna, Veterinärplatz 1, A-1210 Vienna, Austria

^bDepartment of Chemistry, University of Natural Resources and Applied Life Sciences (BOKU), Muthgasse 18, A-1190 Vienna, Austria

Received 20 August 2004; accepted 28 September 2004

Abstract

Free radicals are involved in the onset of many diseases, therefore the availability of adequate spin traps is crucial to the identification and localization of free radical formation in biological systems. In recent studies several hydrophilic compounds of 2-ethoxycarbonyl-2-methyl-pyrroline-*N*-oxide (EMPO) have been found to form rather stable superoxide spin adducts with half-lives up to twenty minutes at physiological pH. This is a major improvement over DMPO ($t_{1/2}$ = ca. 45 s), and even over DEPMPO ($t_{1/2}$ = ca. 14 min), the best commercially available spin trap for the unambiguous detection of superoxide radicals. In order to allow the detection of superoxide and also other radicals in lipid environment a series of more lipophilic derivatives of EMPO was synthesized and their structure unambiguously characterized by ¹H and ¹³C NMR spectroscopy. In this way, six different compounds with a *n*-butyl group in position 5 and either an ethoxy- (EBPO), propoxy- (PBPO), *iso*-propoxy- (*i*PBPO), butoxy- (BBPO), *sec*-butoxy- (*s*BBPO) or *tert*-butoxycarbonyl group (*t*BBPO) in position 5 of the pyrroline ring were obtained and fully analytically characterized (NMR, IR). The stability of the superoxide adducts of all investigated spin traps were comparable with EMPO ($t_{1/2}$ = ca. 8 min), except for the two compounds bearing an additional methyl group in position 3 or 4 of the pyrroline ring, 5-butyl-5-ethoxycarbonyl-3-methyl-pyrroline-*N*-oxide (BEMPO-3) and 5-butyl-5-ethoxycarbonyl-4-methyl-pyrroline-*N*-oxide (BEMPO-4), of which the superoxide adducts were stable for more than 30 min. Spin adducts of other carbon- and oxygen-centered radicals were also investigated.

© 2004 Elsevier Inc. All rights reserved.

Keywords: Spin traps; EPR; Lipophilic EMPO derivatives; Superoxide; Linoleic acid hydroperoxide; Free radicals

1. Introduction

The spin trap EMPO (5-ethoxycarbonyl-5-methyl-1-pyrroline-*N*-oxide) and its derivatives have recently been described by several authors [1–3] to be excellent spin traps for the detection of superoxide radicals. When compared to the structurally related spin traps DMPO

($t_{1/2}$ < 1 min [4]) or EMPO ($t_{1/2}$ = ca. 8 min [5–7]) the compounds bearing bulky substituents on the alkoxy-carbonyl moiety formed considerably more stable superoxide adducts ($t_{1/2}$ = 15–25 min [1,3]) even when compared to the spin trap DEPMPO ($t_{1/2}$ = ca. 14 min [8–10]).

In addition to spin adduct stabilization due to electron-withdrawing as well as steric effects, variation of the 5-alkyl substituent and the 5-alkoxycarbonyl substituents also allows tuning the lipophilic properties of the spin trap. In this regard, the 5-butyl substituent will increase the lipophilicity of the trap. This aspect is of great importance if higher concentrations of the spin trap in a particular biological environment is needed, e.g. within or close to the surface of mitochondrial or other membranes. The two novel compounds BEMPO-3 and BEMPO-4 bear an additional methyl group at position 3 or 4 of the pyrroline ring, thus providing an increased steric shielding effect leading to an even higher stability of the respective superoxide

Abbreviations: BBPO, 5-(butoxycarbonyl)-5-butyl-1-pyrroline-*N*-oxide; DEPMPO, 5-(diethoxyphosphoryl)-5-methyl-1-pyrroline-*N*-oxide; DMPO, 5,5-dimethylpyrroline-*N*-oxide; DTPA, diethylenetriaminepentaacetic acid; EBPO, 5-(ethoxycarbonyl)-5-butyl-1-pyrroline-*N*-oxide; EMPO, 5-(ethoxycarbonyl)-5-methyl-1-pyrroline-*N*-oxide; BEMPO-3, 5-butyl-5-(ethoxycarbonyl)-3-methyl-1-pyrroline-*N*-oxide; BEMPO-4, 5-butyl-5-(ethoxycarbonyl)-4-methyl-1-pyrroline-*N*-oxide; EPR, electron paramagnetic resonance; HFS, hyperfine splitting; LO•, lipoxyl radical; NMR, nuclear magnetic resonance; O₂^{•−}, superoxide anion radical; PBN, *N*-*tert*-butyl- α -phenylnitron; PBPO, 5-(propoxycarbonyl)-5-butyl-1-pyrroline-*N*-oxide; SOD, superoxide dismutase

* Corresponding author. Tel.: +43 1 25077 4400; fax: +43 1 25077 4490.

E-mail address: Hans.Nohl@vu-wien.ac.at (H. Nohl).

adducts. In the present paper we wish to communicate synthesis, analytical properties and spin trapping behavior of a series of substituted pyrroline derivatives with increasing lipophilicity, suitable for the detection of superoxide radicals as well as other oxygen- or carbon-centered radicals in analogy to recently published experiments using peroxidized linoleic acid with the spin traps DMPO [11], DEPMPO [9,10], EMPO [7] and Trazon [12,13].

2. Materials and methods

2.1. Chemicals

Acrolein, croton aldehyde, 2-bromohexanoyl bromide, linoleic acid, methacrolein, superoxide dismutase and xanthine oxidase were commercially available from Sigma-Aldrich. Petroleum ether (high boiling, 50–70 °C) was obtained from Fluka, all other chemicals from Merck.

2.2. Syntheses

Synthesis and characterization of the compounds were performed as reported previously [1,7], in analogy to the synthesis of EMPO and its derivatives [5,6] with minor adaptations as given below.

2.2.1. Alkyl 2-bromohexanoate

2-Bromohexanoyl bromide (70 mmol) was slowly added to a solution of the respective alcohol (100 mmol) and pyridine (70 mmol) in CHCl_3 at 0 °C (ice bath). After stirring for 1 h, the reaction mixture was successively washed with water (50 ml), sulfuric acid (10 %, 50 ml) and concentrated aqueous Na_2CO_3 (50 ml), and dried over Na_2SO_4 overnight. Solvent and excess alcohol were removed under reduced pressure. The crude, nearly colorless product was used without further purification.

2.2.2. Alkyl 2-nitrohexanoate

The respective alkyl 2-bromohexanoate (60 mmol) was added under stirring to a solution of sodium nitrite (7.2 g, 104 mmol) and phloroglucinol dihydrate (8.5 g, 52 mmol) in dry *N,N*-dimethylformamide (120 ml) at room temperature. The solution was stirred overnight, poured into ice water (240 ml), and extracted four times with ethyl acetate (100 ml). The combined extracts were treated twice with 100 ml of saturated Na_2CO_3 solution and dried over Na_2SO_4 . After removal of the solids by filtration, the solvent was evaporated in vacuo. The obtained colorless or pale yellow products were used further without purification.

2.2.3. Alkyl 2-butyl-4-formyl-2-nitrobutanoate

Alkyl 2-nitrohexanoate (23 mmol) was dissolved in a mixture of acetonitrile (10 g, 244 mmol) and triethylamine (0.2 g, 2 mmol). Acrolein (2 g, 38 mmol) was slowly

added at 0 °C. The solution was kept at 10 °C for 1.5 h and then poured into a solution of ice-cold HCl (5 ml of concentrated HCl in 150 ml of water). The solution was extracted three times with CH_2Cl_2 and dried over Na_2SO_4 . After filtration, the mixture was distilled under reduced pressure, and the purity of the remaining product was assessed by thin layer chromatography and IR spectroscopy.

2.2.4. Ethyl 2-butyl-4-formyl-2-nitropentanoate

Same conditions as above, except that methacrolein (2.5 g, 38 mmol) was used instead of acrolein. After slow addition of methacrolein at 0 °C, the solution had to be stirred for several days at room temperature.

2.2.5. Ethyl 2-butyl-4-formyl-3-methyl-2-nitrobutanoate

Same conditions as above, except that croton aldehyde (2.5 g, 38 mmol) was used instead of acrolein. After slow addition of methacrolein at 0 °C, the solution had to be stirred for several days at room temperature.

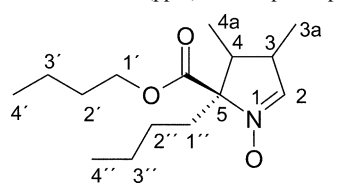
2.2.6. Synthesis of the *N*-oxides

Synthesis of the nitrones was performed according to the procedure described recently for the synthesis of EMPO derivatives [1,7]. To a concentrated solution of 25 mmol of the respective alkyl 2-butyl-4-formyl-2-nitrobutanoate (ethyl 2-butyl-4-formyl-2-nitropentanoate for BEMPO-3; ethyl 2-butyl-4-formyl-3-methyl-2-nitrobutanoate for BEMPO-4) in $\text{H}_2\text{O}/\text{CH}_3\text{OH}$ (*v/v* = 6:4) an aqueous solution of ammonium chloride (1.87 g in 8 ml of water) was added. While zinc dust (8.5 g, 130 mmol) was slowly added within 30 min, the mixture was carefully kept at room temperature. The mixture was stirred for 4.5 h at room temperature, the white precipitate and the remaining zinc powder were removed by filtration, and the residue was washed five times with methanol (30 ml). The liquid phase was concentrated to about 10 ml, saturated with borax and extracted four times with 60 ml CH_2Cl_2 . The organic phase was dried with Na_2SO_4 , filtered and concentrated. Careful purification by column chromatography on silica gel with a petroleum ether/ethanol gradient allowed the separation from the majority of side products and provided the product as a yellow oil or yellow needles. Additional purification was done immediately before the EPR experiments on a 1-ml solid phase extraction column using a Chromabond C-18 100-mg column obtained from Macherey-Nagel (Düren, Germany). The purity of the obtained products was assessed by TLC and UV spectroscopy. Final identification of the purified products was performed by ^1H NMR, ^{13}C NMR, and IR spectroscopy (see Tables 1–3).

2.2.7. Preparation of lipid hydroperoxides

Linoleic acid hydroperoxide was synthesized according to O'Brien [14]. Briefly, linoleic acid was air-oxidized for 72 h in the dark at room temperature. The oxidation

Table 1
¹³C NMR data (ppm) of the spin traps



	² C	³ C	^{3a} CH ₃	⁴ C	^{4a} CH ₃	⁵ C	COO	^{1'} C	^{2'} C	^{3'} C	^{4'} C	^{1''} C	^{2''} C	^{3''} C	^{4''} C
EMPO ^a	134.9	25.4	–	31.9	–	78.5	169.3	61.7	13.4	–	–	20.3	–	–	–
EBPO	135.2	26.0	–	28.3	–	81.8	169.8	61.9	13.7	–	–	32.2	24.8	22.5	13.8
PBPO	135.3	26.1	–	28.4	–	82.0	169.9	67.5	21.8	10.3	–	32.3	24.9	22.6	13.8
<i>i</i> PBPO	135.1	26.1	–	28.4	–	82.0	169.3	69.8	21.5, 21.6	–	–	32.1	24.9	22.7	13.8
BBPO	135.4	26.1	–	28.4	–	82.0	170.0	65.9	30.4	19.0	13.6	32.4	25.0	22.7	13.9
<i>s</i> BBPO	135.3	26.1	–	28.4	–	82.0	169.5	18.9, 19.1	74.2, 74.3	28.4, 28.5	9.4, 9.5	32.3	24.9	22.6	13.8
<i>i</i> BBPO	135.3	26.1	–	28.4	–	82.6	168.6	82.4	27.7	–	–	32.2	25.0	22.7	13.9
<i>t</i> -BEMPO-3	140.2	33.2	18.4	37.2	–	82.7	169.9	62.1	14.0	–	–	32.2	25.1	22.7	13.8
<i>c</i> -BEMPO-3	139.7	33.6	19.1	36.8	–	82.6	170.2	62.1	14.0	–	–	32.7	24.8	22.6	13.8
<i>t</i> -BEMPO-4	134.5	35.0	–	37.2	14.5	84.4	169.9	62.0	14.0	–	–	29.3	26.1	23.0	13.8
<i>c</i> -BEMPO-4	136.4	34.2	–	37.2	15.4	85.1	168.5	61.8	14.1	–	–	30.8	24.8	22.8	13.9

^a Data from Stolze et al. [1].

mixture was dissolved in petroleum ether (boiling range 60–90 °C) and extracted four times with water/methanol (v/v = 1:3). The obtained methanolic phase was counter-extracted four times with petroleum ether (boiling range 60–90 °C) and evaporated under reduced pressure. The obtained hydroperoxide was dissolved in ethanol and stored in liquid nitrogen. The concentration of hydroperoxide was determined by UV spectroscopy based on an extinction coefficient of $\epsilon_{233\text{ nm}} = 25,250\text{ M}^{-1}\text{ cm}^{-1}$ in ethanol [14].

2.3. Instruments

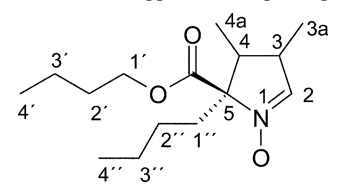
UV–vis spectra were recorded on Hitachi 150-20 and U-3300 spectrophotometers in double-beam mode against a

blank of the respective solvent. Determination of the concentrations was done measuring the absorption maxima in the range between 200 and 350 nm. IR spectra were recorded as film on an ATI Mattson Genesis Series FTIR spectrometer (see also Table 3).

For experiments, Bruker spectrometers (ESP300E and EMX) were used, operating at 9.7 GHz with 100 kHz modulation frequency, equipped with a rectangular TE₁₀₂ or a TM₁₁₀ microwave cavity.

NMR spectra were recorded on a Bruker Avance at 300.13 MHz for ¹H, and 75.47 MHz for ¹³C. CDCl₃ was used as the solvent throughout, TMS (tetramethylsilane) as the internal standard. ¹³C peaks were assigned by means of APT (attached proton test), HMQC (¹H-detected heteronuclear multiple-quantum coherence) and HMBC (hetero-

Table 2
¹H NMR data (ppm) of the spin traps



	² CH=N	³ CH _x	^{3a} CH ₃	⁴ CH _x	^{4a} CH ₃	^{1'} CH _x	^{2'} CH _x	^{3'} CH _x	^{4'} CH ₃	^{1''} CH _x	^{2''} CH _x	^{3''} CH _x	^{4''} CH ₃
EMPO ^a	6.97t	2.75m	–	2.16m, 2.60m	–	4.26m	1.31t	–	–	1.72s	–	–	–
EBPO	6.98t	2.64m, 2.78m	–	2.27m, 2.50m	–	4.26m	1.30t	–	–	2.03m, 2.17m	1.31m	1.40m	0.93t
PBPO	6.99t	2.63m, 2.78m	–	2.27m, 2.50m	–	4.16m	1.69sx	0.95t	–	2.05m, 2.16m	1.30m	1.41m	0.93t
<i>i</i> PBPO	6.91t, 2.76m	2.62m	–	2.27m, 2.46m	–	5.08sp	1.28d	–	–	2.05m, 2.15m	1.31m	1.41m	0.93t
BBPO	7.00t	2.63m, 2.76m	–	2.26m, 2.49m	–	4.19m	1.66qi	1.39m	0.93t	2.05m, 2.16m	1.30m	1.41m	0.93t
<i>s</i> BBPO	7.00t	2.62m, 2.77m	–	2.26m, 2.47m	–	1.25d	4.92sx	1.61m	0.91t	2.03m, 2.14m	1.30m	1.40m	0.93t
<i>i</i> BBPO	6.98t	2.61m, 2.75m	–	2.23m, 2.44m	–	–	1.49s	–	–	1.97m, 2.13m	1.26m	1.37m	0.93t
<i>t</i> -BEMPO-3	6.88t	3.15m	1.19d	1.76dd, 2.64dd	–	4.24m	1.29t	–	–	1.95m, 2.21m	1.30m	1.40m	0.93t
<i>c</i> -BEMPO-3	6.88t	3.02m	1.25d	2.10dd, 2.50dd	–	4.24m	1.30t	–	–	1.95m, 2.21m	1.30m	1.40m	0.92t
<i>t</i> -BEMPO-4	6.96t	2.32m, 2.82m	–	2.96m	1.17d	4.26m	1.30t	–	–	1.96m, 2.23m	1.32m	1.38m	0.93t
<i>c</i> -BEMPO-4	7.00t	2.38m, 2.71m	–	2.71m	1.09d	4.26m	1.30t	–	–	1.96m, 2.23m	1.32m	1.38m	0.93t

Abbreviations: s: singlet; d: doublet; t: triplet; qi: quintuplet; sx: sextet; sp: septet; m: multiplet; dd: doublet of doublets.

^a Data from Stolze et al. [1].

Table 3
IR data (cm⁻¹) of the spin traps

EMPO ^a	2985	2940	2874	1741	1582	1464	1446	1377	1341	1288	1236	1182	1107	1024	950	926	862	796	630
EBPO	2960	2934	2872	1741	1585	1466	1446	1368	1344	1284	1226	1181	1124	1024	939	861	801	774	695
PBPO	2961	2932	2873	1741	1583	1467	1444	1380	1348	1283	1226	1181	1109	1025	993	940	908	799	629
iPBPO	2960	2934	2872	1736	1584	1467	1459	1375	1352	1277	1228	1181	1106	1027	960	938	906	833	632
sBBPO	2960	2932	2873	1741	1584	1466	1459	1381	1343	1278	1225	1181	1122	1023	997	964	940	800	630
sBBPO	2961	2933	2873	1741	1583	1465	1459	1380	1353	1280	1230	1179	1111	1026	996	968	874	852	632
iBBPO	2959	2932	2872	1737	1581	1460	1458	1394	1367	1287	1241	1154	1105	1026	994	954	845	819	631
BEMPO-3	2959	2932	2872	1741	1577	1465	1458	1368	1368	1281	1222	1149	1109	1029	959	859	768	728	699
BEMPO-4	2962	2935	2873	1740	1577	1465	1458	1383	1368	1253	1176	1138	1096	1042	970	902	859	801	746

Intensities: strong (1741), medium (1464), weak (950).

^a Data from Stolze et al. [1].

nuclear multiple bond connectivity) spectra. All chemical shift data are given in ppm units, coupling constants in Hz.

3. Results

3.1. Structure of the spin traps

The identity of the novel spin traps was confirmed by NMR spectroscopy. A complete set of ¹H, H–H correlated, ¹³C, HMQC and HMBC spectra was recorded for each compound, and a full signal assignment for both ¹H and ¹³C was performed. In the current compound series, all derivatives carry a butyl group as 5-substituent, along with a 5-alkoxycarbonyl moiety with varying alkoxy groups. In two compounds, BEMPO-3 and BEMPO-4, an additional methyl substituent was present at C-3 and C-4, respectively. This caused the presence of configurational isomers in these compounds, since the CH₃ group could be arranged either *trans* (*E*) or *cis* (*Z*) to the bulky alkoxy-carbonyl substituent at C-5. Thus, synthesis provided two diastereomers of each spin trap, a *trans*-compound and the respective *cis*-isomer, so that BEMPO-3 and BEMPO-4 were obtained as a mixture of *cis*- and *trans*-isomers in the ratio 45:55 and 35:65, respectively.

Also in the case of sBBPO, two diastereomers were obtained which were not separable by column chromatography, as the C-2' in the 2-butoxy group introduces an additional chiral center into the molecule.

The carbon NMR data of the spin traps confirmed the presence of the pyrroline system, the four signals of the carbons C-2 to C-5 in the heterocyclic ring appearing at averaged values of 135, 26, 28 and 82 ppm. In comparison to EMPO with its 5-methyl substituents, the butyl group in the present series causes a slight downfield shift at C-3 (0.5 ppm), a highfield shift at C-4 (3.5 ppm), and a downfield shift at C-5 (3.5 ppm), cf. Table 1. The resonances of the butyl substituent (C-1'' to C-4'') were found at 32.2, 24.9, 22.6 and 13.9 ppm, respectively. The nature of the alkoxy substituent had no significant effect on the carbon resonances at the pyrroline ring or the butyl group. The effects of additional methyl substituents at either C-3 or C-4, as well as the shifts of the respective *cis*- and *trans*-isomers will not be addressed here, as they are comprehensively covered in a discussion of EDPO derivatives, which will follow this study in due course [15].

Also the ¹H NMR data showed the expected patterns. The geminal protons at H-3, H-4 and H-1'' are diastereotopic and thus magnetically inequivalent caused by the stereogenic center C-5, with shift differences of about 0.14 ppm for H-3, 0.22 ppm for C-4 and 0.12 ppm for H-1''. Similarly, two geminal C-1' protons in alkoxy-carbonyl group at C-5 are diastereotopic, giving a multiplet. As already previously noted [1], the magnetic inequivalence of the two H-3 protons increases with increasing bulkiness of substituents at C-5. Their shift difference is small for 5-

methyl substituents, i.e. in EMPO derivatives, becomes larger (0.04–0.12 ppm) for ethyl and propyl, and reaches approx. 0.14 ppm in the present EBPO derivatives. sBBPO was obtained as a mixture of two diastereomers due to the chiral 2-butoxy substituents, which was introduced as racemic 2-butanol. Only the resonances of the butoxy group showed different ^{13}C resonances, the resonances of the respective other signals of the two isomers were indistinguishable.

As in the case of the ^{13}C resonances, the effect of methyl substituents at C-3 or C-4 on the ^1H spectra shall not be discussed here, as it will be addressed in detail in a following paper [15]. It should just be mentioned that the signal patterns of the H-3 and H-4 protons in the BEMPO-3 and BEMPO-4 derivative showed the expected significant differences in dependence of both substitution site (C-3 or C-4) and configuration (*cis* or *trans*). The *cis/trans*-ratio of BEMPO-3 and BEMPO-4 was easily determined from the integrals in the ^1H spectrum. In BEMPO-3, the proton at C-3 appeared at around 3.10 ppm, and the shift difference between *cis*- and *trans*-isomers was rather small (0.10 ppm). The two geminal H-4 protons appeared at about 2.10/2.50 ppm for the *cis*-compound and 1.76/2.64 ppm for the *trans*-compound. In BEMPO-4, the resonance of H-4 was found at 2.71 ppm for the *cis*-isomers and at 2.96 ppm for the *trans*-isomers. H-4 was thus found more upfield than H-3 in BEMPO-3, and there was a clear difference between *cis*- and *trans*-derivatives in addition. The two geminal H-3 protons appeared at 2.38/2.71 ppm for the *cis*-compound and at 2.32/2.82 ppm for the *trans*-compound. In analogy to the EDPO derivatives, the shift differences of the geminal protons (H-4 in BEMPO-3 and H-3 in BEMPO-4) was much more pronounced for the respective *trans*-isomers. The NMR data are given in Table 1 (^{13}C) and 2 (^1H).

3.2. Spin trapping of superoxide radicals

The general structure of the spin traps is depicted in Fig. 1. In Fig. 2a, the EPR spectrum of the superoxide adduct of EBPO is given as an example. The adduct was generated in the xanthine/xanthine oxidase system at pH 7.4. No EPR spectrum was observed in the presence of SOD (Fig. 2b). Under these conditions similar spectra were obtained from most of the other spin traps, except for BEMPO-3 (Fig. 2c) and BEMPO-4 (Fig. 2d), where additional diastereomeric forms contributed to the observed EPR spectra, some of which were stable for about 30 min. As already shown above for EBPO, no signals were detected in control experiments in which SOD had been added to the incubation mixture prior to xanthine/xanthine oxidase (experiments not shown). Determination of the half-life of superoxide adducts was performed as follows: With the exception of PBPO, the respective spin traps (40 mM in oxygenated phosphate buffer pH 7.4) were pre-incubated for 10 min in the above-mentioned xanthine/xanthine oxidase system, SOD (100 U/ml) was added and the decay of

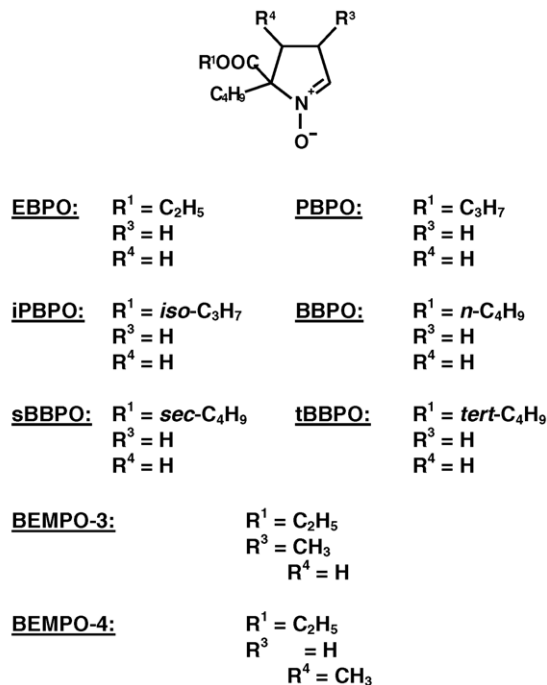


Fig. 1. General structure of the spin traps.

the EPR signal was recorded as a series of consecutive spectra until the superoxide-related lines disappeared and additional lines of lower intensity, consisting mainly of the hydroxyl radical adduct and in some cases a small contribution of a carbon-centered adduct, became predo-

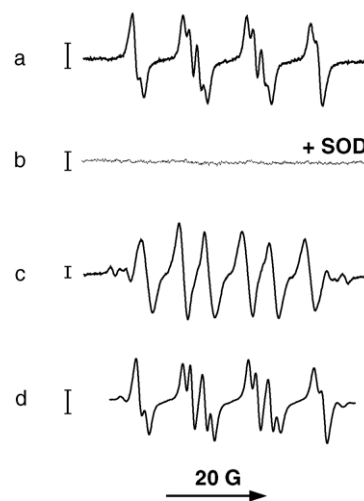


Fig. 2. Formation of the superoxide adducts of the spin traps EBPO, BEMPO-3 and BEMPO-4. (a) EBPO (40 mM), catalase (250 U/ml), xanthine (0.2 mM) and xanthine oxidase (50 mU/ml) in oxygenated phosphate buffer (20 mM, pH 7.4, containing 0.4 mM DTPA) were incubated and measured using the following EPR parameters: sweep width, 60 G; modulation amplitude, 1.0 G; microwave power, 20 mW; time constant, 0.16 s; receiver gain, 2×10^5 ; scan rate, 42.9 G/min. The bars represent 10,000 arbitrary units. (b) Same as in panel a, except that SOD (100 U/ml) was added. (c) Same as in panel a, except that BEMPO-3 (40 mM) was used. (d) Same as in panel a, except that BEMPO-4 (40 mM) was used. EPR parameters: sweep width, 50 G; modulation amplitude, 1.0 G; microwave power, 20 mW; time constant, 0.16 s; receiver gain, 5×10^4 ; scan rate, 35.8 G/min.

Table 4
Half-life of the superoxide adducts and *n*-octanol/buffer partition coefficients of the spin traps

Compound	Apparent $t_{1/2}$ (min)	Partition coefficient <i>n</i> -octanol/phosphate buffer (100 mM, pH 7.0)
EMPO ^a	8.6	0.15
EBPO	4.2	4.92
PBPO	0.36	14.48
<i>i</i> PBPO	15.8	11.79
BBPO	6.4	55.62
<i>s</i> BBPO	6.8	39.03
<i>t</i> BBPO	17.6	22.75
BEMPO-3	47.2	10.84
BEMPO-4	36.2	10.33

^a Data from Stolze et al. [1].

minant. The contribution of these secondary lines was then subtracted from each individual EPR spectrum before calculating the respective half-life. Due to the short half-life of its superoxide adduct, a system using solid KO₂ (ca. 0.5 mg added to 1 ml of an unbuffered aqueous solution) had to be used in the experiments with the spin trap PBPO, immediately followed by addition of SOD

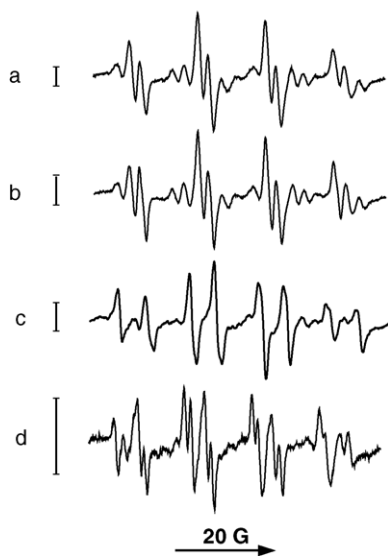


Fig. 3. Formation of hydroxyl radical adducts of the spin traps EBPO, *t*BBPO, BEMPO-3, and BEMPO-4. (a) EBPO (20 mM) was incubated with a Fenton system containing FeSO₄ (1 mM), EDTA (2 mM), H₂O₂ (0.2%). The reaction was stopped after 10 s by 1:1 dilution with phosphate buffer (300 mM, pH 7.4, containing 20 mM DTPA) and the spectrum was recorded using the following spectrometer settings: sweep width, 60.0 G; modulation amplitude, 0.1 G; microwave power, 20 mW; time constant, 0.08 s; receiver gain, 2×10^5 ; scan rate, 42.9 G/min. The bars represent 10,000 arbitrary units. (b) Same conditions, except that *t*BBPO (20 mM) was used. EPR parameters: sweep width, 60 G; modulation amplitude, 0.1 G; microwave power, 20 mW; time constant, 0.08 s; receiver gain, 1×10^5 ; scan rate, 42.9 G/min. (c) Same conditions, except that BEMPO-3 (20 mM) was used. EPR parameters: sweep width, 70 G; modulation amplitude, 0.1 G; microwave power, 20 mW; time constant, 0.08 s; receiver gain, 1×10^5 ; scan rate, 50.1 G/min. (d) Same conditions, except that BEMPO-4 (20 mM) was used. EPR parameters: sweep width, 70.0 G; modulation amplitude, 0.1 G; microwave power, 20 mW; time constant, 0.08 s; receiver gain, 1×10^5 ; scan rate, 50.1 G/min.

(100 U/ml) and catalase (250 U/ml) in phosphate buffer (150 mM, final pH 7.4). With all spin traps the resulting intensity decrease of the first two lines was approximated by a first-order exponential decay, which was in a good agreement with the experimental data. The Pearson correlation coefficient, which characterizes the quality of approximation, was higher than 0.99 for all spin traps investigated, except for EBPO (0.97) and PBPO (0.96). The respective values of apparent superoxide half-lives are listed in Table 4.

3.3. Spin adduct formation with oxygen-containing radicals

EPR spectra of the respective hydroxyl radical adducts were detected in a Fenton system in the presence of the investigated spin traps. Typical EPR spectra are shown in Fig. 3, e.g. from EBPO (Fig. 3a), *t*BBPO (Fig. 3b), BEMPO-3 (Fig. 3c) or BEMPO-4 (Fig. 3d). The EPR spectra of the hydroxyl radical adducts gradually disap-

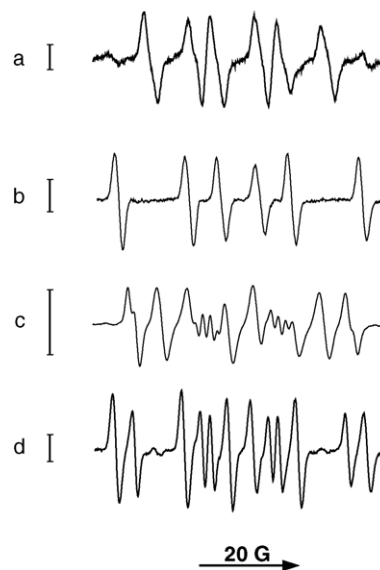


Fig. 4. Iron-dependent formation of spin adducts from methanol and the spin traps EBPO and BEMPO-3. (a) After a 10-s incubation of EBPO (1 M in methanol) with FeCl₃ (2 mM), the reaction was stopped by 1:20 dilution with phosphate buffer (0.3 M, pH 7.4, containing 20 mM DTPA), and the spectrum was recorded with the following spectrometer settings: sweep width, 60 G; modulation amplitude, 0.7 G; microwave power, 20 mW; time constant, 0.08 s; receiver gain, 4×10^5 ; scan rate, 42.9 G/min. The bars represent 10,000 arbitrary units. (b) EBPO (40 mM) was incubated with a Fenton system containing FeSO₄ (1 mM), EDTA (2 mM), H₂O₂ (0.2%) in 10% methanol. The reaction was stopped after 10 s by 1:1 dilution with phosphate buffer (300 mM, pH 7.4, containing 20 mM DTPA) and the spectrum was recorded using the following spectrometer settings: sweep width, 70 G; modulation amplitude, 0.1 G; microwave power, 20 mW; time constant, 0.08 s; receiver gain, 1×10^5 ; scan rate, 50.1 G/min. (c) Same conditions as in a), except that BEMPO-3 was used. Sweep width, 60 G; modulation amplitude, 0.7 G; microwave power, 20 mW; time constant, 0.08 s; receiver gain, 8×10^4 ; scan rate, 171.8 G/min. (d) Same conditions as in panel b, except that BEMPO-3 was used. Sweep width, 70 G; modulation amplitude, 0.1 G; microwave power, 20 mW; time constant, 0.08 s; receiver gain, 1×10^5 ; scan rate, 50.1 G/min.

Table 5
Comparison of the EPR parameters of different radical adducts of various lipophilic EMPO derivatives

Radical HFS (G)	EMPO ^a	EBPO	PBPO	iPBPO	BBPO	sBBPO	tBBPO	BEMPO-3	BEMPO-4
•OOH	(43%) (57%)	(37%) (63%)	(42%) (58%)	(37%) (63%)	(37%) (63%)	(37%) (63%)	(37%) (63%)	(63%) (25%) (12%)	(60%) (40%)
<i>a</i> ^N	13.28 13.28	13.20 13.18	13.21 13.21	13.20 13.22	13.22 13.24	13.25 13.20	13.28 13.28	12.95 13.40 13.40	13.45 13.45
<i>a</i> ^H	9.67 11.89	9.12 11.60	9.35 11.54	9.20 11.80	9.14 11.70	9.20 11.75	9.12 11.79	7.50 14.50 17.00	10.80 7.90
•OH	(50%) (50%)	(45%) (55%)	(45%) (55%)	(45%) (55%)	(45%) (55%)	(42%) (58%)	(38%) (62%)	(71%) (29%)	(55%) (45%)
<i>a</i> ^N	14.00 14.00	14.05 13.93	14.12 13.93	14.07 13.90	14.01 13.86	14.05 13.87	14.10 13.93	13.75 14.30	13.80 13.80
<i>a</i> ^H	15.00 12.58	15.89 12.21	16.02 12.21	15.93 12.15	15.80 12.08	15.89 12.09	16.00 12.20	8.70 19.20	11.00 8.80
	0.90	(0.65) (0.80)	(0.65) (0.80)	(0.65) (0.80)	(0.65) (0.80)	(0.65) (0.80)	(0.65) (0.80)	(0.85)	
•H	(100%)	(100%)	(100%)	(100%)	(71%) (29%)	(82%) (18%)	(100%)	(70%) (30%)	(90%) (10%)
<i>a</i> ^N	15.52	15.34	15.32	15.37	15.35 15.20	15.32 15.22	15.42	15.20 15.40	15.40 15.20
<i>a</i> ^H	22.21	22.94	22.99	22.92	22.95 25.20	22.98 25.23	22.96	16.45 17.45	17.60 18.45
<i>a</i> ^H	20.82	19.92	19.88	19.93	19.98 17.35	19.93 17.33	20.04	26.36 24.90	26.00 23.96
•CH₃	(100%)	(100%)	(40%) (60%)	(36%) (64%)	(26%) (74%)	(29%) (71%)	(18%) (82%)	(46%) (42%) (12%)	(59%) (41%)
<i>a</i> ^N	15.42	14.75	15.20 15.12	15.25 15.25	15.10 15.13	15.21 15.22	15.21 15.32	15.25 15.10 15.35	15.20 15.00
<i>a</i> ^H	22.30	21.48	21.10 23.80	24.30 21.65	24.25 21.34	24.10 21.35	24.38 21.38	26.60 15.75 18.40	17.75 19.30
•OCH₃	(50%) (50%)	(56%) (44%)	–	–	(47%) (53%)	–	(47%) (53%)	(60%) (21%) (19%)	(70%) (23%) (7%)
<i>a</i> ^N	13.74 13.74	13.45 13.45	–	–	13.45 13.45	–	13.50 13.50	13.45 13.80 13.90	13.38 14.71 13.87
<i>a</i> ^H	10.87 7.81	10.42 7.62	–	–	10.56 7.62	–	10.90 8.10	5.70 15.10 17.50	7.33 18.89 17.97 1.45
•CH₂OH	(100%)	(100%)	(100%)	(100%)	(100%)	(56%) (44%)	(58%) (42%)	(56%) (44%)	(100%)
<i>a</i> ^N	14.95	14.80	14.83	14.83	14.84	14.87 14.75	14.82 15.02	14.86 14.66	14.76
<i>a</i> ^H	21.25	21.44	21.31	21.39	21.28	20.40 22.35	21.45 20.45	24.60 16.80	18.79
•C(LOOH)	(62%) (38%)	(60%) ^b	(53%) ^b	(58%) ^b	(45%) ^b	(46%) ^b	(62%) ^b	(30%) ^b (30%) ^b	(100%)
<i>a</i> ^N	13.45 13.45	15.00	14.70	14.95	14.80	15.00	15.00	15.00 14.10	15.00
<i>a</i> ^H	11.45 8.55	21.70	22.00	21.90	21.95	22.10	21.50	24.20 19.20	18.80

^a Data from Stolze et al. [7].

^b Rest mainly •OH-adduct.

peared within about 15–20 min with concomitant formation of hitherto unidentified secondary products.

Two simple model systems were chosen to discriminate between the formation of oxygen-centered and carbon-centered radical adducts from alcohols such as methanol:

Fe³⁺-catalyzed formation of alkoxy radical adducts according to Dikalov and Mason [11], leading to the short-lived EBPO/•OCH₃ adduct (Fig. 4a), and the Fenton system containing 5% methanol described by Roubaud et al. [16], giving rise to the more stable EBPO/•CH₂OH spin adduct (Fig. 4b), of which the observed HFS values (*a*^N = 14.80 G; *a*^H = 21.44 G) are clearly different from those of the methoxy radical adduct (*a*^N = 13.45 G; *a*^H = 10.42 G; 56% and *a*^N = 13.45 G; *a*^H = 7.62 G; 44%). The compounds BEMPO-3 and BEMPO-4 possess two asymmetric C-centers, therefore the formation of different diastereomers upon radical trapping can be expected. In Fig. 4c, the EPR spectra of the two stereoisomeric forms of BEMPO-3/•OCH₃ are shown, and the EPR spectrum of BEMPO-3/•CH₂OH can be seen in Fig. 4d. The spectral contribution of the different isomers was assessed by computer simulation (see Table 5).

3.4. Spin trapping of lipid-derived free radicals

We also investigated radicals formed in a Fenton-type reaction from peroxidized linoleic acid in the presence of Fe²⁺ [11,12]. Under anaerobic conditions a mixture of

several radicals was observed with EBPO (Fig. 5a), whereas in oxygenated buffer mainly the EBPO hydroxyl radical adduct was observed (Fig. 5b). A rather complex mixture of radicals was observed when BEMPO-3 was used (Fig. 5c). With BEMPO-4 on the other hand, only one species predominated the spectrum, most probably a lipid-derived carbon-centered radical adduct (Fig. 5d). The spectral parameters of lipid-derived adducts of the other spin traps are listed in Table 5.

4. Discussion

Eight derivatives of the spin trap EMPO were synthesized in this study, which possess increased lipophilicity due to a butyl side chain at C-5. All compounds were comprehensively analytically characterized, and a full NMR assignment (¹H, ¹³C) was performed. The two substances with an extra methyl group in position 3 (BEMPO-3) and 4 (BEMPO-4) of the pyrroline ring form very stable superoxide adducts (*t*_{1/2} = ca. 36–47 min), at least 30 times more stable than the respective adducts with DMPO (*t*_{1/2} = 45 s) [4] and approximately two times more stable than superoxide adducts of DEPMPO derivatives (*t*_{1/2} = ca. 7–15 min [8–10]). This stabilizing effect is most probably due to steric shielding rather than electronic influences as has already been mentioned previously [1].

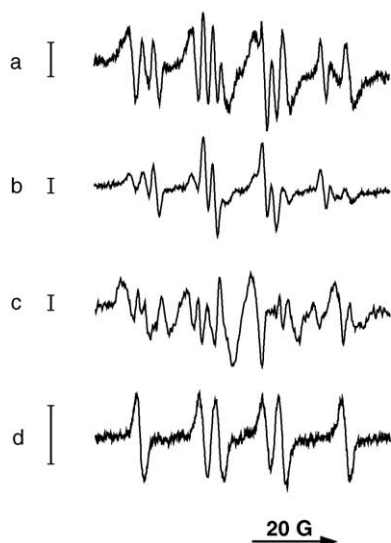
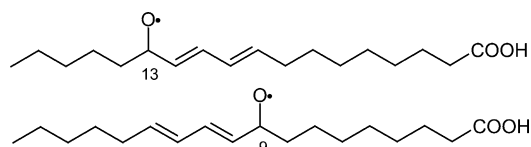


Fig. 5. Detection of a lipid-derived radical adduct from peroxidized linoleic acid using a Fenton-type incubation system in the presence of the spin traps EBPO, BEMPO-3 or BEMPO-4. (a) To a nitrogen-bubbled solution of peroxidized linoleic acid (1 mM) and EBPO (40 mM) in phosphate buffer (10 mM, pH 7.4) FeSO_4 (0.2 mM) was added and the spectrum was recorded with the following spectrometer settings: sweep width, 80.0 G; modulation amplitude, 1 G; microwave power, 20 mW; time constant, 0.08 s; receiver gain, 2×10^5 ; scan rate, 57.2 G/min, 6 scans accumulated. The bar represents 10,000 arbitrary units. (b) Same conditions as in panel a, except that the solution was oxygen bubbled. Sweep width, 80.0 G; modulation amplitude, 1 G; microwave power, 20 mW; time constant, 0.08 s; receiver gain, 1×10^5 ; scan rate, 57.2 G/min, 6 scans accumulated. The bar represents 10,000 arbitrary units. (c) Same conditions as in panel a, except that BEMPO-3 (20 mM) was used. Sweep width, 100.0 G; modulation amplitude, 1 G; microwave power, 20 mW; time constant, 0.16 s; receiver gain, 5×10^5 ; scan rate, 71.5 G/min, 20 Scans accumulated. The bar represents 10,000 arbitrary units. (d) Same conditions as in panel a, except that BEMPO-4 (20 mM) was used. Sweep width, 70.0 G; modulation amplitude, 0.1 G; microwave power, 20 mW; time constant, 0.08 s; receiver gain, 2.5×10^4 ; scan rate, 50.1 G/min. The bar represents 1000 arbitrary units.

Determination of the half-lives of the superoxide adducts was done using a first-order exponential decay approximation (Pearson correlation coefficient $r^2 > 0.99$, except for EBPO (0.97) and PBPO (0.96)). Under the experimental conditions used a second order decay of the superoxide adducts was insignificant. An important issue to consider is the fact that the observed spectral intensity does not only depend on the half-life of the spin adducts, but also on the rate constant of the spin trapping reaction, the spectral line width, the total number of lines, and additional factors, such as enzyme binding or the solubility (aggregate formation) of the spin trap, reduction by antioxidants or buffer constituents, and degradation by transition metal catalyzed reactions (Fenton-type reactions, oxidation by Fe^{3+} , etc.). In view of these facts the half-life values given in Table 4 are therefore to be interpreted only as preliminary, and further tests will be necessary to test these compounds in different biological systems.

Sufficiently stable alkoxy radical adducts were only obtained from EBPO, BBPO, *t*BBPO, BEMPO-3 and

BEMPO-4, which gave the respective methoxyl radical adducts that rearranged within several minutes into the respective carbon-centered adducts. Furthermore, in the experiments performed with peroxidized linoleic acid carbon-centered radical adducts were also detected (under anaerobic conditions). Whether originally trapped oxygen-centered radical adducts rearranged rapidly into the respective carbon-centered form or whether the originally formed alkoxy radicals underwent rapid β -scission (rate constant ca. 10^6) prior to radical trapping cannot be decided. A variety of secondary reactions has been reported leading to carbon-centered radicals according to different pathways [17] involving intermediates such as LOO^\bullet [18–23] or LO^\bullet . Most probably the oxygen in the primary alkoxy radical formed from peroxidized linoleic acid is located either in position 9 or 13, as shown in the following figure.



In conclusion, the two ring-methylated EMPO derivatives BEMPO-3 and BEMPO-4 can be recommended for trapping of superoxide radicals, since the half-life of their superoxide adducts is about 36–47 min. Moderately stable hydroxyl radical adducts were detected from all spin traps investigated, but the stability of alkoxy radical adducts, such as the methoxyl radical adduct, was rather low, and most of these adducts rearranged into the more stable hydroxymethyl radical adduct.

From these results it can be concluded that minor changes of the geometry around the attack site of the radical have a profound influence on the spin adduct stability as well as the EPR spectral shape. More detailed studies covering compounds bearing substituents in positions 3 or 4 of the pyrroline moiety will therefore be conducted in the near future.

Acknowledgements

The authors wish to thank R. Stadtmüller for skilful technical assistance in synthesis, purification, and characterization of the spin traps. The present study was supported by the Austrian Fonds zur Förderung der wissenschaftlichen Forschung.

References

- [1] Stolze K, Udilova N, Rosenau T, Hofinger A, Nohl H. Synthesis and characterization of EMPO-derived 5,5-disubstituted 1-pyrroline-*N*-oxides as spin traps forming exceptionally stable superoxide spin adducts. *Biol Chem* 2003;384:493–500.
- [2] Zhao H, Joseph J, Zhang H, Karoui H, Kalyanaraman B. Synthesis and biochemical applications of a solid cyclic nitron spin trap: a relatively superior trap for detecting superoxide anions and glutathyl radicals. *Free Radic Biol Med* 2001;31:599–606.

- [3] Tsai P, Ichikawa K, Mailer C, Pou S, Halpern HJ, Robinson BH, et al. Esters of 5-carboxyl-5-methyl-1-pyrroline-*N*-oxide: a family of spin traps for superoxide. *J Org Chem* 2003;68:7811–7.
- [4] Buettner GR, Oberley LW. Considerations in the spin trapping of superoxide and hydroxyl radical in aqueous systems using 5,5-dimethyl-1-pyrroline-1-oxide. *Biochem Biophys Res Commun* 1978;83:69–74.
- [5] Olive G, Mercier A, LeMoigne F, Rockenbauer A, Tordo P. 2-Ethoxycarbonyl-2-methyl-3,4-dihydro-2*H*-pyrrole-1-oxide: evaluation of the spin trapping properties. *Free Radic Biol Med* 2000;28:403–8.
- [6] Zhang H, Joseph J, Vasquez-Vivar J, Karoui H, Nsanzumuhire C, Martásek P, et al. Detection of superoxide anion using an isotopically labeled nitron spin trap: potential biological applications. *FEBS Lett* 2000;473:58–62.
- [7] Stolze K, Udilova N, Nohl H. Spin adducts of superoxide, alkoxy, and lipid-derived radicals with EMPO and its derivatives. *Biol Chem* 2002;383:813–20.
- [8] Fréjaville C, Karoui H, Tuccio B, Le Moigne F, Culcasi M, Pietri S, et al. 5-(Diethoxyphosphoryl)-5-methyl-1-pyrroline-*N*-oxide: a new efficient phosphorylated nitron for the in vitro and in vivo spin trapping of oxygen-centered radicals. *J Med Chem* 1995;38:258–65.
- [9] Stolze K, Udilova N, Nohl H. Spin trapping of lipid radicals with DEPMPO-derived spin traps: detection of superoxide, alkyl and alkoxy radicals in aqueous and lipid phase. *Free Radic Biol Med* 2000;29:1005–14.
- [10] Stolze K, Udilova N, Nohl H. Lipid radicals: properties and detection by spin trapping. *Acta Biochim Pol* 2000;47:923–30.
- [11] Dikalov SI, Mason RP. Spin trapping of polyunsaturated fatty acid-derived peroxy radicals: reassignment to alkoxy radical adducts. *Free Radic Biol Med* 2001;30:187–97.
- [12] Stolze K, Udilova N, Nohl H. ESR analysis of spin adducts of alkoxy and lipid-derived radicals with the spin trap Trazon. *Biochem Pharmacol* 2002;63:1465–70.
- [13] Sankuratri N, Janzen EG. Synthesis and spin trapping chemistry of a novel bicyclic nitron: 1,3,3-trimethyl-6-azabicyclo[3.2.1]oct-6-ene-*N*-oxide (Trazon). *Tetrahedron Lett* 1996;37:5313–6.
- [14] O'Brien PJ. Intracellular mechanisms for the decomposition of a lipid peroxide. I. Decomposition of a lipid peroxide by metal ions, heme compounds, and nucleophiles. *Can J Biochem* 1969;47:485–92.
- [15] Stolze K, Udilova N, Rosenau T, Hofinger A, Stadtmüller R, Nohl H, unpublished results.
- [16] Roubaud V, Lauricella R, Bouteiller JC, Tuccio B. *N*-2-(2-Ethoxycarbonyl-propyl)- α -phenylnitron: an efficacious lipophilic spin trap for superoxide detection. *Arch Biochem Biophys* 2002;397:51–6.
- [17] Rota C, Barr DP, Martin MV, Guengerich FP, Tomasi A, Mason RP. Detection of free radicals produced from the reaction of cytochrome P-450 with linoleic acid hydroperoxide. *Biochem J* 1997;328:565–71.
- [18] Van der Zee J, Barr DP, Mason RP. ESR spin trapping investigation of radical formation from the reaction between hematin and *tert*-butyl hydroperoxide. *Free Radic Biol Med* 1996;20:199–206.
- [19] Akaie T, Sato K, Ijiri S, Miyamoto Y, Kohno M, Ando M, et al. Bactericidal activity of alkyl peroxy radicals generated by heme-iron-catalyzed decomposition of organic peroxides. *Arch Biochem Biophys* 1992;294:55–63.
- [20] Kalyanaraman B, Mottley C, Mason RP. A direct ESR and spin-trapping investigation of peroxy free radical formation by hematin/hydroperoxide systems. *J Biol Chem* 1983;258:3855–8.
- [21] Chamulitrat W, Takahashi N, Mason RP. Peroxy, alkoxy, and carbon-centered radical formation from organic hydroperoxides by chloroperoxidase. *J Biol Chem* 1989;264:7889–99.
- [22] Davies MJ. Detection of peroxy and alkoxy radicals produced by reaction of hydroperoxides with heme-proteins by ESR spectroscopy. *Biochim Biophys Acta* 1988;964:28–35.
- [23] Davies MJ. Detection of peroxy and alkoxy radicals produced by reaction of hydroperoxides with rat liver microsomal fractions. *Biochem J* 1989;257:603–6.